Stabilization mechanism of Si_{12} cage clusters by encapsulation of a transition-metal atom: A density-functional theory study

Noriyuki Uchida
Advanced Semiconductor Research Center, National Institute of Advanced Industrial Science and Technology, 1-1-1 Higashi, Tsukuba, Ibaraki 305-8562, Japan
and Institute of Applied Physics, University of Tsukuba, 1-1-1 Tenoudai, Tsukuba, Ibaraki 305–8573, Japan

Takehide Miyazaki
Research Institute for Computational Sciences, National Institute of Advanced Industrial Science and Technology, 1-1-1 Umezono, Tsukuba, Ibaraki 305-8568, Japan

Toshihiko Kanayama
Advanced Semiconductor Research Center, National Institute of Advanced Industrial Science and Technology, 16-1 Onogawa, Tsukuba, Ibaraki 305-8569, Japan

(Received 18 May 2006; revised manuscript received 18 July 2006; published 22 November 2006)

We systematically studied the geometrical and electronic structures of transition-metal (M)-encapsulating Si_{12} cage clusters, MSi_{12} (M=Hf, Ta, W, Re, Os, Ir, Pt, and Au), mainly focusing on their outstanding stability, using calculations based on density-functional theory. We found that the MSi_{12} clusters except $HfSi_{12}$ belong to either of two distinct structural classes, the D_{6h}-symmetric hexagonal prism (HP; for M=Ta, W, Re, and Os; total number of valence electrons per cluster, N_v, ranging from 53 to 56) and less-symmetric four pentagonal face (FPF; M=Re, Os, Ir, Pt, and Au; N_v ranging from 55 to 59) structures. The HP structure is particularly stabilized at N_v=54, which is understood in terms of the electronic shell closure of the M atoms due to the 18-electron rule, and the geometrical symmetry is maintained for N_v=53, 55, and 56 by the covalent bonding between the M atom and the Si cage accompanied by the cage-to-M charge transfer. The FPF structure is lowest in energy for N_v=56 and is maintained by the same covalent-bond/charge-transfer mechanism for other values of N_v. We propose that all these results originate from the electronic "rigidness" of the HP and FPF Si cages against the variation of N_v, which is the leading factor governing the stability of MSi_{12}.

DOI: 10.1103/PhysRevB.74.205427 PACS number(s): 36.40.Qv, 31.10.+z, 61.48.+c, 31.15.Ew

I. INTRODUCTION

Atomic clusters often exhibit particular stability when they take peculiar structures that never form in bulk materials. The most remarkable examples are the cage clusters such as fullerenes composed purely of carbon atoms, in which the constituent atoms are topologically arranged on a sphere surface. Since the discovery of C_{60}, the cage cluster has been attracting a vast range of interest because of its structural completeness as a building unit of nanoscale materials and structures.[1] The cage structure has also the advantage that its hollow structure allows additional atoms to be contained in the cluster, thereby tailoring the properties.

Cage clusters made of Si have also been pursued by theoretical and experimental approaches because Si is the most important material in modern semiconductor device technology. One of the consequences is that such cage structures as fullerenes are difficult to form purely with Si atoms because Si does not favor the sp^2 hybridization that carbon favors.[2] Instead, Si cage clusters can be synthesized by adding suitable foreign atoms to terminate dangling bonds of Si, which inherently arise in cagelike networks. In fact, the $Si_{29}H_{24–36}$ cluster was reported[3] to have a cage structure owing to the termination of dangling bonds by the hydrogen atoms.

Alternatively, the inclusion of a transition metal (M) atom has also been reported to stabilize Si cage structures by internally terminating dangling bonds.[4,5] The M-doped Si clusters, MSi_n, were synthesized by laser vaporization[6,7] and an ion-trap method.[4,8] The results indicated that the MSi_{12} and $MS_{15,16}$ clusters are relatively stable compared to other compositions. Theoretical calculations[5,9–21] suggested that these clusters have M-encapsulating Si cage structures. In particular, the MSi_{12} cluster has a unique Si cage network with a hexagonal prism (HP) structure [Fig. 1(a)],[5,11–19] while the Si cages of the $MSi_{15,16}$ clusters form fullerenelike spherical structures.[9,10]

In this paper, we address the outstanding stability of the MSi_{12} clusters. Up to now, numerous theoretical results for the ground-state HP cage structures have been presented for the 3d metal atoms (M=Ti, V, Cr, Mn, Fe, Co, Ni, and Cu),[12,13,15–18] the 4d metal atoms (M= Zr, Nb, and Mo)[11,14] and the 5d metal atoms (M=Hf, Ta, W, Re, Pt, and Au).[5,11,14,15] As an experimental manifestation of the structural toughness of HP-cage MSi_{12}, the HP-shaped cagelike structures have been observed with scanning tunneling microscopy (STM) on the Si(111)-(7×7) surfaces where the $TaSi_{12}$ clusters were deposited.[8] Moreover, the presence of an M-doped Si nanotube composed of the units of M-encapsulating HP MSi_{12} clusters was theoretically predicted, and related structures were actually observed on Si (111) surfaces.[16,19,20] The latter experiment implies that the MSi_{12} cluster may be a potential candidate for a constructive unit of Si-based nanomaterials owing to its stability.

Nevertheless, the reason for this outstanding stability of the MSi_{12} clusters has not been fully understood yet. A pos-

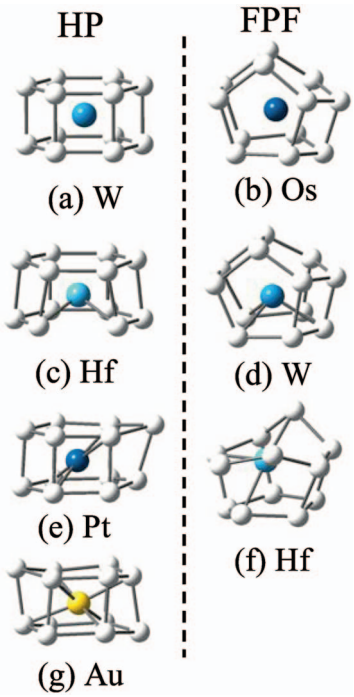

FIG. 1. (Color) Converged structures of MSi_{12} clusters calculated using GAUSSIAN 03 B3PW91/LanL2DZ: (a) WSi_{12} with the symmetrical (D_{6h}) HP Si_{12} cage structure, (b) $OsSi_{12}$ with the symmetrical FPF Si_{12} cage structure, (c) $HfSi_{12}$ with a distorted HP structure, (d) WSi_{12} with a distorted FPF structure, (e) $PtSi_{12}$ with a distorted HP structure, (f) $HfSi_{12}$ with a distorted FPF structure, and (g) $AuSi_{12}$ with a distorted HP structure. The white balls represent Si atoms, and the blue and yellow ones are M atoms.

sible hypothesis for the stability is the formation of a rare-gas-atomlike closed electronic shell in those clusters. In a case of the 5*d* transition metal atoms (M=Ta, W, Re, and Ir), Hiura *et al.*[4] have found in their ion-trap experiment that the MSi_n clusters lose their reactivity with silane SiH_4 molecules if the sum of the atomic number of M and the number of the Si atoms (n) is equal to 86, which is the atomic number of Rn. For example, n is twelve for M=W (the atomic number is 74). Based on this result, they conjectured that the stability of MSi_n (M=Ta, W, Re, and Ir) originates from the valence electron-shell closure of the M atom with 18 electrons (the 18-electron rule), in which the valency of M is 18-n and one valence electron per Si is provided by the Si cage. Especially, when M=W (n=12), each of the twelve Si atoms may be threefold coordinated to each other to form an HP cage containing the W atom inside the cage, leaving no unsaturated Si dangling bonds.

To test the above conjecture of the 18-electron rule, some theoretical studies have been performed, mainly focusing on the role of the *d* electrons of transition-metal atoms in stabilization of the clusters. Khanna *et al.*[12] have found that the $CrSi_{12}$ cluster favors the HP Si cage, where Cr belongs to the 3*d* series. They have compared the binding-energy gains between the incremental reactions $Si_{12}+Si \rightarrow Si_{13}$ and $Si_{12}+Cr \rightarrow CrSi_{12}$, and found that the energy gain of the latter is substantially larger than the former. Since a Cr atom has six valence electrons, Khanna *et al.*[12] have concluded that for $CrSi_n$ the number n=12 is magic due to the creation of a closed 18-electron shell. They further have found that for the $CrSi_n$ clusters (n=11, 12, 13, and 14) the magnetic moment of Cr is completely quenched due to strong hybridization of Cr 3*d* with 3*s* and 3*p* states of Si.

However, Sen and Mitas[14] have claimed the 18-electron rule is just one of the aspects that determine the cluster stability. Indeed they have found that the formation energy of $CrSi_{12}$ is not the highest one in the 3*d* series and also that neither the $ReSi_{11}$ (Re belongs to the 5*d* series) nor $FeSi_{10}$ (Fe belongs to the 3*d* series) clusters, which both have the 18 valence electrons, are energetically favorable because the former is less stable than $ReSi_{12}$ and the latter has a very small binding energy. Sen and Mitas have pointed out that the hybridization of the *d* orbitals of a transition-metal atom and the *p* orbitals of the HP Si cage becomes stronger when the transition-metal atom gets heavier ($3d \rightarrow 4d \rightarrow 5d$). In other words, there are two factors to enhance the *p*-*d* hybridization between the HP Si cage and a heavy transition-metal atom: (i) the larger size of the transition-metal atoms fits the hexagonal cavity better, (ii) for heavier transition-metal atoms, the atomic levels become shallower and energetically closer to the *p* levels of Si.

Later, Reveles and Khanna[13] have revisited the validity of the 18-electron rule for the MSi_{12} clusters with various M atoms belonging to the 3*d* series. They have enforced the spin conservation (the Wigner-Witmer rule[21]) to evaluate the binding energy of a MSi_{12} cluster against fragmentation to M and Si_{12} and found that the binding energies of $CrSi_{12}$ and $FeSi_{12}$ are highest among the 3*d* series. They have attributed the stability of these clusters to the generation of the closed 18-electron ($1s^21p^61d^{10}$) and 20-electron ($1s^21p^61d^{10}2s^2$) shells, respectively. The authors[13] have also calculated the binding energies of MSi_{12} clusters with the 5*d* M atoms according to the Wigner-Witmer rule and found that they exhibit maxima at M=W (18 electrons) and M=Os (20 electrons). The binding energy maxima at M=W and M=Os are in agreement with the study by Sen and Mitas,[14] who use the Hund rule without spin conservation.

Alternatively, Andriotis *et al.*[17] and Mpourmpakis *et al.*[18] have argued the stability of MSi_{12} (M=V or Ni) in the light of the relationship between the occupation in the *d* shell of an M atom and the coordination number of the ligands connecting to M. They have found that VSi_{12} has the HP Si cage but the Si atoms in $NiSi_{12}$ are arranged in a spherical geometry with C_{5v} symmetry. This difference in the bonding properties have been understood from the analogy to the contrasting bonding behaviors of $V_x(C_{60})_2$ and $Ni_x(C_{60})_2$ (Refs. 22 and 23): For x=1 (x=2), the C_{60} cluster acts as the η^6 ($\eta^3$and η^4) ligands for V and as the η^2 (η^2 and η^3) ligands for Ni, where η^k means that the ligand has k bonds to the M atom.

A crucial criterion for the validity of the 18- or 20-electron rule for MSi_{12} is the symmetry of the cluster structure. In principle, the electron-shell picture may apply best when a system of interest has a spherical symmetry. In reality, this "ideal" electron-shell structure has to be perturbed according to the lower symmetry of the cluster structure. In order to assess the validity of the electron-counting rules for MSi_{12}, one should explicitly explain how the geometry of a cage affects the electronic structure of the cluster as a whole.

This is our standpoint, which may augment the above previous studies to yield a deeper understanding of the peculiar stability of the MSi_{12} clusters.

Yet another crucial point in the assessment of the electron-counting rules for MSi_{12} is that one should study as many topological variations of the Si cage as possible. All of the above theories have assumed that the HP Si cage structure is the only generic structure for the stable form of the MSi_{12} cluster except $NiSi_{12}$.[17] However, not only the HP cage but also the one with the four pentagonal faces (FPF) (Ref. 5) [Fig. 1(b)] may give rise to a stable form of MSi_{12}. The FPF structure is composed of four pentagons and four squares and is a structural isomer of the HP counterpart. These two structures are topographically similar to each other in that both of them are classified as simple 3-polytopes, i.e., polyhedrons composed of 12 vertices, 18 edges, and 8 faces. Among them, the regular HP structure maximizes the number of inner diagonals running close to the M atom in the Si_{12} cage.[5]

Keeping the above in mind, the purpose of this work is to systematically study the effect of the cage geometry on the electronic properties and, hence, the stability of the MSi_{12} clusters. For that purpose, we investigated stable structures and electronic structures of MSi_{12} clusters with the HP and FPF Si cages for the 5d transition metals, M (= Hf, Ta, W, Re, Os, Ir, Pt, and Au), using density-functional calculations. In particular, we examined the bonding states between the M atoms and Si_{12} cages and the relation between the number of valence electrons of a cluster and the structure of the Si_{12} cage.

II. CALCULATION METHOD

All calculations were carried out based on density-functional theory using the GAUSSIAN 03 package.[24] The electronic structure calculations were performed with both the B3PW91 (Refs. 25 and 26) and B3LYP (Refs. 27 and 28) exchange-correlation functionals. We did not find significant differences in any of the calculation results between these functionals. The molecular orbitals of clusters were constructed with the LanL2DZ, SDD, and SDDAll basis sets.[24] The B3PW91 and B3LYP functionals are hybridizations of Becke's three-parameter functional and the nonlocal correlation functional. The Perdew 91 and Lee-Yang-Parr expressions were provided as nonlocal correlation functionals. The LanL2DZ basis set[29–31] uses the Dunning/Huzinaga full double zeta basis[32] for the first-row elements and the Los Alamos effective core potentials (ECP) plus double-zeta basis for Na–Bi. The SDD basis set uses the Dunning/Huzinaga full double zeta basis up to Ar and Stuttgart/Dresden ECP[33–35] for other atoms in the periodic table except for Fr and Ra. When we use the SDDAll basis set, the Stuttgart/Dresden ECP is selected for all atoms that have atomic number of $Z>2$ except Fr and Ra.

Projector augmented-wave (PAW) method[36] would be a more accurate approximation than the ECP for any system, in the sense that by using the PAW method the valence wave functions with correct nodal structures can be constructed and even the atomic core wave functions in the clusters could also be obtained if needed. However, the use of the PAW method is not urgently necessary for our present purpose. As we shall see later, the calculated relative formation energies (ΔE_f, see caption of Table I for definition) of the clusters except $OsSi_{12}$ converge with respect to the ECP basis set as well as the DFT functional (see Table I). As for $OsSi_{12}$, it is sufficient at present to know that the formation energy of this cluster is nearly degenerate between HP and FPF.

TABLE I. Difference of E_f between the HP and FPF structures [$\Delta E_f = E_f$(HP)–E_f(FPF)] using two functionals (B3PW91 and B3LYP) with three basis sets (LanL2DZ, SDD, and SDDAll).

Method	WSi_{12}	$OsSi_{12}$	$PtSi_{12}$	$AuSi_{12}$
B3PW91/LanL2dz	−1.239	−0.058	1.112	0.369
B3LYP/LanL2dz	−1.197	−0.114	1.014	0.345
B3PW91/SDD	−1.242	0.033	0.801	0.463
B3PW91/SDDAll	−1.476	−0.215	0.820	0.507

The total energy per cluster converged within $\approx 4.3 \times 10^{-2}$ eV in each self-consistent-field run. We calculated the total energy including the zero point energy. Structure optimization of MSi_{12} clusters was performed using the GDIIS algorithm,[37] starting from several initial structures, which were the regular HP and the symmetrical FPF, and other structures discussed later. Because the structures of the clusters to be optimized were only perturbations of either HP or FPF, we found that the GDIIS algorithm worked very efficiently throughout the structure optimization process. When the maximum atomic force in the cluster became less than 0.03 eV/Å, the structure optimization was terminated.

III. RESULTS

A. Stable structures of MSi_{12} clusters

We obtained the optimized structures for the MSi_{12} clusters for 5d transition metal atoms, M (= Hf, Ta, W, Re, Os, Ir, Pt, and Au), starting from either the symmetrical HP with D_{6h} symmetry or the FPF. The optimized structures for M=Hf, W, Os, Pt, and Au are shown in Fig. 1. As is evident in the figure, all these clusters have geometries belonging to *either* the HP family or the FPF family, suggesting that the two prototypical topologies of the Si cage exhibit particular stability when they enclose the 5d transition metals. The structure converged to the HP similar to the initial structure with D_{6h} symmetry [Fig. 1(a)] when Ta–Os atoms were encapsulated in the cage, while the Si_{12} cage was deformed for M=Hf [Fig. 1(c)] and Ir–Au [Figs. 1(e) and 1(g)]. FPF structures [Fig. 1(b)] were observed as optimized structures for M=Re–Au. As seen in Figs. 1(d) and 1(f), the FPF structure was also deformed by the encapsulation of Hf–W atoms.

To confirm the particular stability of the HP and FPF structures, we looked for other possible structures of MSi_{12} clusters. Examples of converged structures, $S1$–$S4$, are shown in Fig. 2. It is known that when an alkali metal atom is doped into Si_n clusters, the alkali metal atom is not included in the inside but adsorbed outside the Si_n

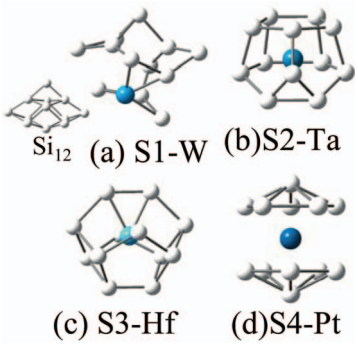

FIG. 2. (Color) Examples of converged structures of MSi_{12} clusters other than HP and FPF structures: (a) WSi_{12} with the $S1$ structure and the lowest-energy structure of the Si_{12} cluster (b) $TaSi_{12}$ with the $S2$ structure (c) $HfSi_{12}$ with the $S3$ structure, and (d) $PtSi_{12}$ with the $S4$ structure.

frameworks.[38] Accordingly, we performed structure optimization starting from the Si_{12} framework reported by Liu[39] on which an M atom adsorbed. A converged structure of the Si_{12} cluster adsorbed with a W atom is shown in Fig. 2(a). As seen, the original Si_{12} network was partly broken by the W

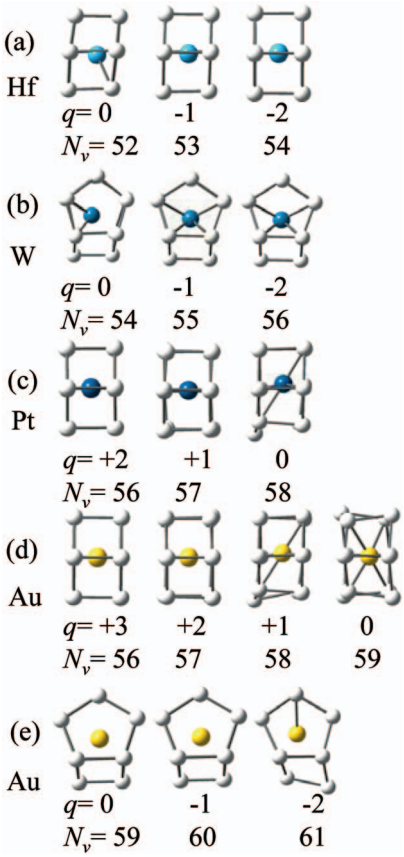

FIG. 3. (Color) Structures of MSi_{12} clusters in positively or negatively charged states: (a) $HfSi_{12}$ with the HP structure, (b) WSi_{12} with the FPF structure, where the W atom is not located at the cage center for $q=0$, (c) $PtSi_{12}$ with the HP structure, (d) $AuSi_{12}$ with the HP structure, and (e) $AuSi_{12}$ with the FPF structure. The q value represents the charge state for each of the cluster ions. The N_v is total number of valence electrons.

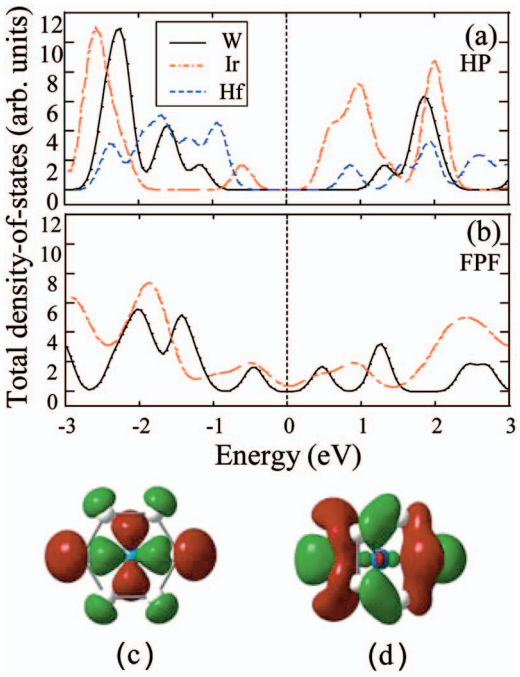

FIG. 4. (Color) Total density of state (DOS) of the MSi_{12} clusters (M=Hf, W, and Ir) (a) for the HP structure, and (b) for the FPF structure. The DOS data are presented in a continuous Gaussian-band shape plot of 0.2 eV in standard deviation. The Fermi level corresponds to 0 eV on the energy axis. The wave functions contributing to the covalent bonds between the M atom and the Si_{12} cage are also shown: (c) a wave function of WSi_{12} with the HP structure at −2.29 eV of the eigenenergy and (d) a wave function of $IrSi_{12}$ with the FPF structure at −1.99 eV of the eigenenergy. The red and green lobes show wave functions with opposite phases.

adsorption. Similar dissociation of the Si_{12} framework was observed in the case of adsorption of other 5d transition metal atoms. Other converged structures are shown in Figs. 2(b)–2(d). We found a type of Si_{12} cage of a simple 3-polytope structure, $S2$ [Fig. 2(b)], starting from a heuristically formed cage, which includes a three-membered ring of Si atoms in addition to four- to six-membered rings. The resulting $S2$ structure preserves the original topology, and the converged structures are similar for all the 5d transition metals. Another converged structure, $S3$ [Fig. 2(c)], was already reported as a basketlike structure of WSi_{12}.[4] The $S3$ structure appeared for the encapsulation of Hf–Os atoms, while this structure was converted into FPF for the encapsulation of Ir–Au. On the other hand, icosahedral packing is a typical structure of metal clusters composed of 12 and 13 atoms. Thus, we performed structure optimization for M encapsulation in the icosahedral Si_{12} cage. We found that the encapsulation of Pt or Au dissociates the icosahedron into a capped structure, $S4$ [Fig. 2(d)], while the Si_{12} cage is converted into HP or FPF for M=Hf–Ir.

B. Total valence electron number of MSi_{12}

The deformation of the Si cage mentioned above is strongly correlated with the "fluctuation" (deficiency or excess) of the total number of the valence electrons (N_v) in

MSi_{12}, around the "special numbers": 54 and 56 for the regular HP (D_{6h}) and FPF Si cages, respectively. Here, N_v is defined as the sum of four valence electrons from each Si atom and the number of 6*s* and 5*d* electrons of the *M* atom. The "special" N_v values (54 and 56) are those at which the formation energy of the MSi_{12} cluster are concave with respect to the variation of N_v (Fig. 5). We find that the MSi_{12} cluster forms well-defined HP (FPF) Si cages in a *certain range* of N_v, 53–56 (55–59). Substantial distortion of the both Si cages occurs outside of the respective N_v ranges. For example, in the case M=Hf, which has only two 5*d* and two 6*s* electrons, i.e., N_v=52, both the HP and FPF structures are deformed by the deficiency in the valence electrons. Another example is that, when the Ir–Au atoms, which have seven to ten 5*d* electrons and one or two 6*s* electrons (N_v=57–59), are encapsulated into the HP structure, the Si_{12} cage are deformed owing to the excess valence electrons.

Apart from changing the *M* atoms as above, the fluctuation of N_v can also be introduced by changing the charge states of clusters with *M* unchanged. As shown in Figs. 3(a) and 3(b), the symmetry of both the HP cage with Hf and FPF cage with W is restored by the charging of the clusters at a singly or doubly negative state. The N_v values of HP $HfSi_{12}^-$ and FPF WSi_{12}^- clusters are 53 and 55, respectively. This indicates that N_v=53 and 55 are the lower limits to form the symmetrical HP with D_{6h} symmetry and FPF structures, respectively. On the other hand, the $IrSi_{12}$ (N_v=57), $PtSi_{12}$ (N_v=58), and $AuSi_{12}$ (N_v=59) clusters cannot form the symmetrical HP structure because they contain more electrons than N_v=56. As shown in Figs. 3(c) and 3(d), the D_{6h} HP structure is again restored for the cationic clusters of $PtSi_{12}^{2+}$ and $AuSi_{12}^{3+}$, all of which have N_v of 56. The HP $OsSi_{12}$ cluster (N_v=56) deformed similarly to the HP $IrSi_{12}$ cluster (N_v=57) by an electron capture to $OsSi_{12}^-$. This shows that the upper limit of N_v is 56 to form the symmetrical D_{6h} HP structure. For the FPF structure, the upper limit of N_v is 60 because the deformation of this structure occurred only for the $AuSi_{12}^{2-}$ anion, as shown in Fig. 3(e). Thus, we have determined that the range of N_v required for the formation of the symmetrical HP structure of D_{6h} is from 53 to 56, and that for the FPF is from 55 to 60. The FPF structure can take in larger values of N_v than the HP structure without the substantial Si cage deformation.

This difference in the ranges of N_v values to form the symmetrical HP and FPF Si_{12} cages originates from the difference in the electronic states between these two motif structures. To observe the difference, we plotted the total density of states (DOS) near the edges of occupied and unoccupied states of the MSi_{12} clusters (M= Hf, W, and Ir) for the HP and the FPF structures in Fig. 4. In the HP case, we observe a highest occupied molecular orbital-lowest unoccupied molecular orbital (HOMO-LUMO) gap of 2.6 eV for the encapsulation of a W atom, while narrower HOMO-LUMO gaps are found for deformed structures with Hf and Ir owing to the generation of midgap levels [Fig. 4(a)]. This shows that the D_{6h} HP structure has a rigid electronic structure. To characterize the rigidness of the electronic structures quantitatively, we evaluated the chemical hardness, η, of MSi_{12} clusters, defined as η=(IP–EA)/2, where IP is the ionization potential of the clusters, and EA is the electron affinity. The larger the η value, the more rigid the electronic structure and hence the narrower the window of the N_v values to maintain the symmetrical Si cages. The η value is 2.46 eV for the symmetrical $HPWSi_{12}$ and is larger than those of deformed $HfSi_{12}$ (1.90 eV) and $IrSi_{12}$ (1.79 eV), indicating the stronger rigidness of the electronic structure of D_{6h} HP WSi_{12}. The narrow range of N_v for the symmetrical HP structure is due to the rigidness of electronic structure. On the other hand, the DOS distributions for WSi_{12} and $IrSi_{12}$ with the FPF structure [Fig. 4(b)] are relatively continuous near the HOMO and LUMO, and hence, the HOMO-LUMO gap is narrow compared to that of the HP structure. Actually, η for FPF WSi_{12} is 1.73 eV. For this reason, the Si_{12} cage with the FPF structure can take in excess 5*d* and 6*s* electrons from the *M* atom without causing significant structural deformation. Figures 4(c) and 4(d) show representative wavefunctions of WSi_{12} with the HP structure at −2.29 eV of the eigenenergy and $IrSi_{12}$ with the FPF structure at −1.99 eV of the eigenenergy in occupied states. We observe in Figs. 4(c) and 4(d) the overlap between the *d* orbitals of the *M* atom and the *s*/*p* orbitals of the Si atoms. This shows that the covalent bonds are efficiently formed between the *M* atoms and the Si_{12} cages. These symmetrical wave functions indicate that the 5*d* orbitals of the *M* atoms are favorable to form the bonds with the HP and FPF Si cages.

C. Formation energy and embedding energy of MSi_{12}

To compare the stability of these structures quantitatively, we calculated the formation energy, E_f, defined as

$$E_f = E(MSi_{12}) - E(M) - 12E(\mathrm{Si}),$$

where $E(MSi_{12})$ is the total energy of the MSi_{12} cluster, and $E(M)$ and E(Si) are the total energies of the *M* and Si atoms. The results are shown in Fig. 5. In the evaluation of $E(M)$ and $E(MSi_{12})$, the spin multiplicity was optimized to obtain the ground-state energy in each case. The ground states of free Si and *M* atoms were identified by Hund's rules as follows: a spin doublet for Au; a spin triplet for Si, Hf, and Pt; a spin quartet for Ta and Ir; a spin quintet for W and Os; and a spin sextet for Re. The ground state is the spin singlet for the $HfSi_{12}$, WSi_{12}, $OsSi_{12}$, and $PtSi_{12}$ clusters, while it is the spin doublet for $TaSi_{12}$, $ReSi_{12}$, $IrSi_{12}$, and $AuSi_{12}$. Reveles and Khanna[13] pointed out that the Wigner-Witmer rule must be adopted to obtain proper values of the dissociation energy of the clusters. To calculate E_f, the Wigner-Witmer rule requires that the *M* atom has the same spin multiplicity with the MSi_{12}. We also calculated E_f using the E(M) of the spin singlet for Hf, W, Os, and Pt, and spin doublet for Ta, Re, Ir, and Au. Our results support their view in that the E_f values calculated by the Wigner-Witmer rule are distributed in the range 0.51–3.52 eV lower than those by Hund's rule for the MSi_{12} (M=Hf–Pt) clusters. However, both the rules give the same dependence of stability on structure, while the Wigner-Witmer rule emphasizes the stability of the WSi_{12}, $ReSi_{12}$, and $OsSi_{12}$ clusters with both the HP and FPF structures. This result strongly suggests the electron-shell closure as a

physical reason for the stability of the $M\mathrm{Si}_{12}$ clusters, which we will discuss in Sec. IV B in detail. As seen in Fig. 5, E_f of the HP or FPF structure calculated by Hund's rule is 0.69–1.36 eV lower than that of the S1–S4 structures. For Hf–Os, the HP is the lowest energy structure, while for Ir–Au, the FPF is lower in E_f than the HP, indicating that the HP Si_{12} cage is less favorable for encapsulation of Ir–Au atoms than the FPF Si_{12} cage. This is consistent with the deformation of HP for Ir–Au seen in Fig. 1. We observed even-odd oscillations of E_f depending on N_v for M=Ta–Ir. The E_f is lowest for the encapsulation of W, Re, and Os, which have nearly half occupation of the d orbitals and fully occupied 6s orbitals. Eventually, the W-doped HP structure is most stable in the Si_{12} cages encapsulating 5d transition metal atoms.

To investigate why E_f depends on the encapsulated M atom species, we calculated the embedding energy, E_e, of the M atom into the Si_{12} cage as

$$E_e = E(M\mathrm{Si}_{12}) - E(M) - E_M(\mathrm{Si}_{12}),$$

where $E_M(\mathrm{Si}_{12})$ is the total energy of the $M\mathrm{Si}_{12}$ cluster from which the M atom is taken out, leaving the Si_{12} cage structure intact. The value of E_e reflects the strength of interaction between the M atom and the Si_{12} cage. We see in Fig. 5 that E_e behaves quite similarly to E_f for both the HP and FPF structures. This indicates that the stability of the clusters is mainly determined by the interaction of the encapsulated M atom with the Si cage. Here, we compare the HP and the FPF quantitatively in the inset of Fig. 6 by looking at the differences in E_f and E_e, ΔE_f and ΔE_e, the values of the HP structure measured relative to those of the FPF. The ΔE_f is ≈ -1 eV for M=Hf–W, indicating that the HP is more stable than the FPF at this value. The ΔE_f corresponds approximately to the ΔE_e, indicating that the difference of E_f between the HP and FPF structures is mainly determined by the difference of E_e.

For OsSi_{12}, the ΔE_f has much smaller absolute value than those for the other clusters. In order to assess the reliability of the ΔE_f values, we repeated structure optimization and calculation of ΔE_f for M= W, Os, Pt, and Au by changing the DFT functionals (B3PW91 and B3LYP) as well as the ECP basis sets (LanL2dz, SDD, and SDDAll). The result is shown in Table I. In order to determine the sign of ΔE_f of OsSi_{12}, it should be necessary to employ a more accurate basis set such as PAW. However, it is sufficient for our present interest to know that the formation energies of OsSi_{12} with the HP and FPF structures are close to each other.

D. Natural population analysis of the M-cage bonds

To elucidate the nature of the covalent bonds between the M atom and the Si atoms, we performed natural population analysis (NPA),[40] a part of natural bond orbital (NBO) analysis.[41] NPA is an appropriate method of investigating the bonding nature because it is based on the evaluation of charge population of each of the bonding orbitals. The NPA analysis enabled us to estimate the relative electron densities on the encapsulated M atoms in terms of the natural charge (NC). As seen in Fig. 7, the NC density on the M atoms except Au was negative owing to electron transfer from the Si_{12} cage. Hagelberg *et al.*[15,16] reported the similar result that the NCs on the W and Cu atoms of the HP structure are −1.74 and 0.48 e, respectively. The FPF Si_{12} cage delivers a larger number of electrons to the encapsulated M atom than the HP structure does. The amount of NC on the metal atom increases with the decreasing atomic number of the M species except Hf, in other words, with decreasing N_v. In particular, in the range where the HP and FPF Si_{12} cages keep the symmetry, NC is directly proportionate to N_v, as indicated by the straight lines in Fig. 7. Comparing the slopes of the two lines, we see that the NC of FPF increases more rapidly than that of HP. This illustrates that the FPF cage more favorably compensates for the variation of N_v by electron transfer than the HP and is consistent with the fact that the HP structure has a more rigid electronic structure than the FPF counterpart. As discussed above, the range of N_v required to form the symmetrical HP of D_{6h} is 53–56, and for FPF, N_v=55–60. For these ranges of N_v, the symmetrical structures can be maintained by the electron transfer from the Si_{12} cage to the M atom even if the 5d and 6s electrons of the M atom are too few to make the bonding complete.

Note that the observed dependence of NC on N_v is opposite to that of the electronegativity. For example, Ta acquires the largest density of electrons, although it has a smaller electronegativity than any of W–Au. This trend indicates that the electron transfer from the Si cage to the M atom is induced when the N_v is not large enough to make sufficient covalent bonds between the cage and the M atom. We observed a lower electron density on Hf than Ta despite the number of valence electrons of Hf being smaller than that of Ta. This is caused by the structure deformation of the Si_{12} cage seen in Fig. 1. In fact, the NCs on the Hf atom are estimated as −2.21 and −2.47 e, even larger than those of Ta, if the symmetrical HP of D_{6h} and FPF structures are forcibly preserved. The number of electrons in the HfSi_{12} cluster is too small to form the symmetrical HP of D_{6h} and FPF structures.

IV. DISCUSSION

A. Role of the electronic structure of Si_{12} cages in stabilization of $M\mathrm{Si}_{12}$

Here we will clarify the effect of the Si cage structure of $M\mathrm{Si}_{12}$ on its electronic structure. For this purpose, we tried to abstract the Si_{12}-cage states from the $M\mathrm{Si}_{12}$ clusters. Since dangling bonds of the Si_{12} cages were terminated by the encapsulated M atom, hydrogenation of the Si_{12} cages is one method to mimic the Si_{12} cages in the $M\mathrm{Si}_{12}$ clusters. Therefore, we calculated the energy levels of the model clusters, the $\mathrm{Si}_{12}\mathrm{H}_{12}$ cages with HP and FPF structures. The use of the model clusters simplifies the relation between the stability of $M\mathrm{Si}_{12}$ clusters and the electronic structures of Si_{12} cages. The Si atoms are arranged to mimic the structures of WSi_{12} with HP cage and OsSi_{12} with FPF cage. The electronic structures of these model clusters are obtained by optimizing the positions of the H atoms while those of the Si atoms are fixed.

The distributions of the eigenstates of HP and FPF hydrogenated Si_{12} cages are shown in Fig. 8(a). As seen in Fig.

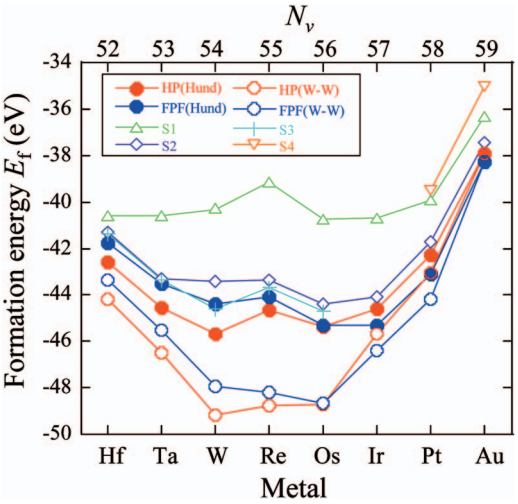

FIG. 5. (Color) The formation energy, E_f, of MSi_{12} clusters for M=Hf–Au with HP, FPF, and $S1$–$S4$ structures. For HP and FPF, two different calculation methods for spin multiplicity (Hund's and Wigner-Witmer rules) are compared, while for $S1$–$S4$ the values calculated by Hund's rule are shown.

8(a), many levels of the HP(W) are degenerate owing to the D_{6h} symmetry, while the FPF(Os) has only one degenerate level. The LUMO level of the HP(W) is not degenerate and thus can accommodate two excess electrons without changing the structure, making the D_{6h} HP structure stable for Re and Os in addition to W; i.e., the maximum value of N_v is 56. On the other hand, for FPF, the LUMO+1 level of FPF(Os) is found below the LUMO of HP(W). This shows that the FPF favorably admits four excess electrons at the LUMO and LUMO+1. This is consistent with the fact that the upper limit of N_v to form the symmetrical FPF structure is 60, larger than that of 56 for the HP.

The LUMO+1 of HP(W) is a doubly degenerate level. Accordingly, when M=Ir and N_v=57 for the D_{6h} HP structure, an additional electron must be populated into the LUMO+1, but the actual result is that the LUMO+1 splits

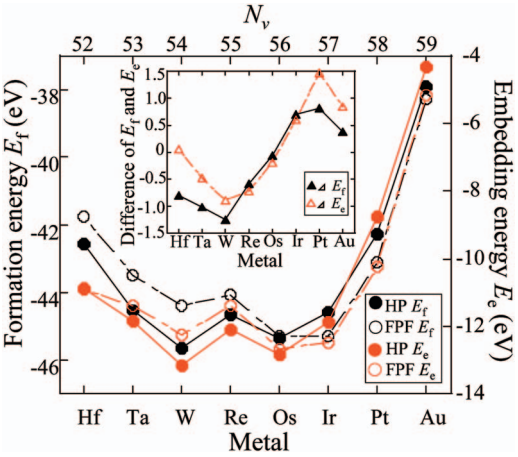

FIG. 6. (Color) Formation energy, E_f, and embedding energy, E_e, for the HP and FPF structures of MSi_{12} clusters for M=Hf–Au. The inset shows the differences in E_f and E_e, ΔE_f, and ΔE_e, the values of the HP structure measured from those of the FPF.

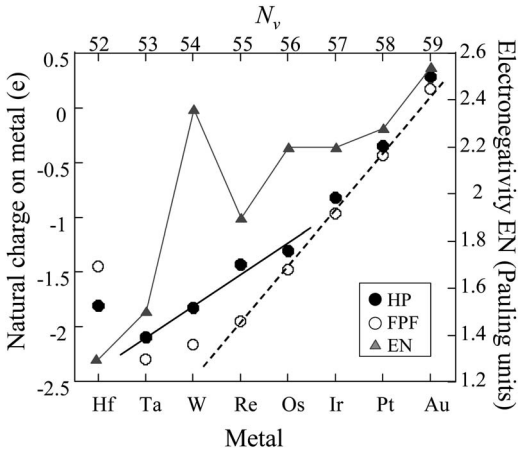

FIG. 7. The natural charge on the encapsulated M atom in HP and FPF MSi_{12} clusters (M=Hf–Au) and Pauling electronegativity (EN) (Ref. 42) of the M atoms.

[Fig. 8(b)], leading to a deformation by the Jahn-Teller effect. Similarly, the HOMO of HP(W) is also a doubly degenerate level. Thus, when two electrons are deficient as in the case of HP(Hf), the HOMO level splits by the Jahn-Teller effect, resulting in a deformation. These vulnerability of the structure to the N_v variation indicates that the HP $Si_{12}H_{12}$ clusters have rigid electronic structures. In contrast, the de-

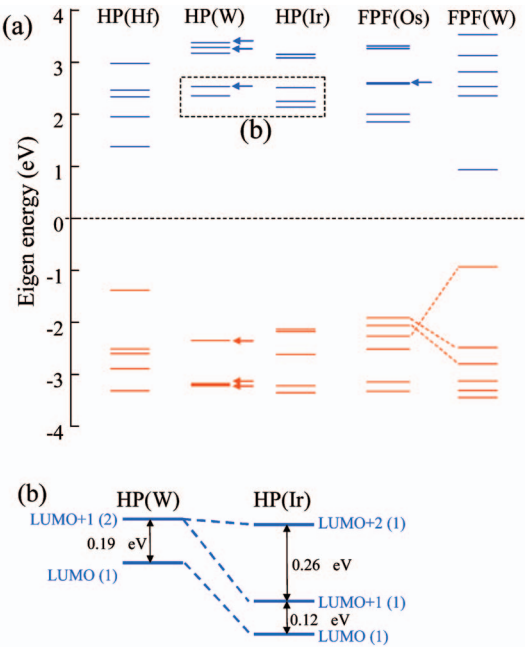

FIG. 8. (Color) (a) The distribution of the eigenvalues of the $Si_{12}H_{12}$ clusters having the same structures as the MSi_{12} clusters. The HP(M) and FPF(M) denote the $Si_{12}H_{12}$ clusters in which the Si atoms take the same positions as in the HP and FPF MSi_{12} clusters and the positions of 12 hydrogen atoms are optimized. The red and blue bars show the occupied and unoccupied states, respectively. The arrows show degenerate levels. The broken lines connecting the levels between FPF(Os) and FPF(W) indicate that each pair of connected levels have similar orbital symmetry. (b) Magnified diagram of area (b) in (a).

formation of FPF(W) is not caused by the Jahn-Teller deformation because the HOMO and HOMO–1 levels of the FPF(Os) are not degenerate. Instead, the HOMO–2 level of the FPF(Os) is promoted to the midgap level in FPF(W) to accommodate hole states resulting from encapsulation of the W atom, as shown in Fig. 8(a). Note that the hydrogenation of the Si_{12} cages does not affect the above discussion because the molecular orbitals near the HOMO and LUMO levels are not localized on a particular Si atom but widely distributed on the whole Si bonding network.

B. The closed electron-shell picture of the stability of $M\mathrm{Si}_{12}$

Finally, we would like to comment on the usefulness of the 18- and 20-electron rules to model the electronic structure of $M\mathrm{Si}_{12}$, where the 5*d* transition metals are encapsulated in HP and FPF structures. Reveles and Khanna[13] concluded that the 18- and 20-electron rules are applicable to the Si_{12}-cage cluster encapsulating the 3*d* transition metal assuming the Wigner-Witmer rule. We also obtained the same results for the 3*d* and 4*d* transition metals, but as shown in the above sections, the stability at 18 and 20 electrons holds for $M=5d$ transition metals both with the Wigner-Witmer and the Hund rules. This indicates that the 18- and 20-electron rules are more clearly applied to the $M\mathrm{Si}_{12}$ clusters encapsulating the 5*d* transition metal than the case of the 3*d* and 4*d* transition metals.

On the other hand, Sen and Mitas[14] have denied the 18-electron rule using a quantum Monte Carlo calculation, because the $ReSi_{11}$ cluster, which has the 18 valence electrons, has smaller binding energy than the $ReSi_{12}$. For the structure of $ReSi_{11}$ they assumed that the Re atom is sandwiched between a Si pentagonal ring and a hexagonal ring. Obviously, the symmetry of this cluster is so low that the 18-electron rule does not apply to this cluster. As will be mentioned below, the geometrical symmetry of a cluster is a crucial factor in determining the validity of the electron-counting picture for that cluster.

It should be stressed that the 18- and 20-electron rules are rather insensitive to the precise geometric and electronic structures of a given cluster but instead very sensitive to the symmetry of the cluster, if the size of the cluster is small. We can consider the valence electrons in the $M\mathrm{Si}_{12}$ clusters as a confined electron gas in spite of the efficient covalent bonding between the *M* atom and the Si cage because the spatial extension of the molecular orbitals is nearly the same as the size of the cluster, owing to the smallness of the $M\mathrm{Si}_{12}$ cluster. In such a situation, the "envelope functions" of the molecular orbitals are not essentially different from those of the wave functions for a confined electron gas. This physical insight is evidenced by a theoretical work by Manninen *et al.*[43] They concluded that electronic-shell structures are derived both from a tight-binding cluster and from a confined free-electron cluster, and the low-energy density of states of two types clusters are equivalent to each other. The HP and FPF cage structures have symmetries high enough for the well-defined shells to evolve.

Figure 5 shows that the W-doped HP Si_{12} cluster is most stable among the $M\mathrm{Si}_{12}$ clusters encapsulating the 5*d* transition metal. Several authors[4,12,13] attributed the stability of the WSi_{12} cluster to the 18-electron rule. The W atom in the WSi_{12} cluster possesses 18 electrons, which is the sum of six valence electrons of the W atom and 12 electrons from the Si_{12} cage, assuming that each Si atom of the cluster supplies a single electron to the central W atom to form covalent bonds between the W atom and the Si cage. Confined in the symmetrical HP structure of D_{6h}, the 18 electrons make the closed electronic-shell structure of $1s^2 1p^6 1d^{10}$, resulting in a particularly stable electronic state, where nl^x (e.g., $1s^2$) represents the occupation of shell states in the cluster. In addition, the 20-electron system may make an electronic closed-shell structure of $1s^2 1p^6 1d^{10} 2s^2$, as highlighted by Reveles and Khanna.[13] Turning to the $OsSi_{12}$ cluster, which has 20 valence electrons (eight from the Os and 12 from the cage), the HP and FPF cages are both favored (Fig. 5), suggesting the occurrence of the $1s^2 1p^6 1d^{10} 2s^2$ configuration in both the cages.

Our calculation results show that both the 18- and 20-electron systems are stabilized in the HP cage but only the 20-electron system in the FPF cage. The latter is caused by lower symmetry in the FPF than in the HP cage. In principle, a spherical symmetry gives the ideal condition to the shell structure, in which the angular momentum is a relevant quantum number to represent the degeneracy. Up to 20 electrons, there are the 1*s*, 1*p*, 1*d*, and 2*s* occupied shells with proper degeneracy. When the symmetry lowers, the degenerate shell structures are split off. In the case of HP (D_{6h}) structure, the splitting is small enough to establish the shell structures consisting of the 18 or 20 electrons. The symmetry of the FPF structure is D_{2d} at most, causing a further *d*-level splitting relative to D_{6h}. However, the FPF structure is more geometrically spherelike in comparison with the HP cage, which has two open hexagonal faces, leading to the lower 2*s* level than that in the HP structure. Therefore, the 1*d* and 2*s* levels get close to each other in energy, and hence are viewed as one shell in the FPF structure, suggesting that the 18-electron rule becomes unclear but a clear shell closure occurs at 20 electrons. This is why the 18- and 20-electron rules are applied to HP structure but only the 20-electron rule in FPF structure.

V. CONCLUSIONS

We have thoroughly investigated the structure, energetics, and bonding nature of neutral and charged $M\mathrm{Si}_{12}$ clusters with the HP and FPF Si cages, where *M* represents the 5*d* transition metals (M=Hf–Au), using density-functional calculations. A main message from our results is that the shape of a Si_{12} cage (HP or FPF) plays a key role in determining the structural stability because the stable structure of the cluster is governed by cooperative interplay between two factors, which are both sensitive to the cage structure: (i) the covalent bonding between the Si_{12} cage with electron transfer and (ii) the rigidness of the electronic structure of the Si_{12} cage. In particular, we demonstrated the relation between the structure of a Si_{12} cage and the number of valence electrons in a $M\mathrm{Si}_{12}$ cluster, N_v. The HP structure is lower in energy for N_v=52–56 than the FPF. The HP of N_v=54 and the FPF

of N_v=56 are most stable because the 18- and 20-electron rules are applicable. The HP and FPF structures are preserved for N_v=53–56 and 55–60, respectively, while theSi_{12} cage is deformed when N_v is out of these ranges. These tolerable ranges of N_v are determined by how many electrons more or less than N_v=54 and 56 are accommodated in the Si_{12} cage. The rigid electronic structure of the HP cage narrows the N_v range compared to the FPF cage.

Additionally, the 18- and 20-electron counting rules are applicable to the HP and FPF Si_{12} cages encapsulating the 5 *d* transition metal. Both the 18- and 20-electron systems may be stabilized in the HP cage but only the 20-electron system in the FPF cage. The latter is caused by the lower symmetry in the FPF than in the HP cage.

Note added in proof. Recently, electron counting rules were examined for cationic, neutral, and anionic MSi_{15}, MSi_{16}, and MSi_{17} (M=Sc, Ti, and V) clusters by Reveles and Khanna.[44] They concluded that the stability of MSi_n clusters is enhanced by the 20 electron rule.

ACKNOWLEDGMENT

This work was partly supported by the Japan Society for the Promotion of Science (JSPS), Grant-in Aid for Scientific Research (A) 16201026 (2004).

[1] R. E. Smally and B. I. Yakobson, Solid State Commun. **107**, 597 (1998).
[2] M. Broyer *et al.*, in *Cluster Assembled Materials*, edited by K. Sattler, Vol. 232 (Trans Tech Publications, Zurich-Utikon, 1996), p. 27.
[3] G. Belomion, J. Therrien, A. Smith, S. Rao, R. Twesten, S. Chaieb, M. H. Nayfeh, L. Wagner, and L. Mitas, Appl. Phys. Lett. **80**, 841 (2002).
[4] H. Hiura, T. Miyazaki, and T. Kanayama, Phys. Rev. Lett. **86**, 1733 (2001).
[5] T. Miyazaki, H. Hiura, and T. Kanayama, Phys. Rev. B **66**, 121403(R) (2002).
[6] S. M. Beck, J. Chem. Phys. **87**, 4233 (1987).
[7] M. Ohara, K. Koyasu, A. Nakajima, and K. Kaya, Chem. Phys. Lett. **371**, 490 (2003).
[8] N. Uchida, L. Bolotov, T. Miyazaki, and T. Kanayama, J. Phys. D **36**, L43 (2003).
[9] V. Kumar and Y. Kawazoe, Phys. Rev. Lett. **87**, 045503 (2001).
[10] V. Kumar, C. Majumder, and Y. Kawazoe, Chem. Phys. Lett. **363**, 319 (2002).
[11] T. Miyazaki, H. Hiura, and T. Kanayama, Eur. Phys. J. D **24**, 241 (2003).
[12] S. N. Khanna, B. K. Rao, and P. Jena, Phys. Rev. Lett. **89**, 016803 (2002).
[13] J. U. Reveles and S. N. Khanna, Phys. Rev. B **72**, 165413 (2005).
[14] P. Sen and L. Mitas, Phys. Rev. B **68**, 155404 (2003).
[15] J. Han, C. Xiao, and F. Hagelberg, Struct. Chem. **13**, 173 (2002).
[16] C. Xiao, F. Hagelberg, and W. A. Lester, Jr., Phys. Rev. B **66**, 075425 (2002).
[17] A. N. Andriotis, G. Mpourmpakis, G. Froudakis, and M. Menon, New J. Phys. **4**, 78 (2002).
[18] G. Mpourmpakis, G. Froudakis, A. N. Andriotis, and M. Menon, J. Chem. Phys. **119**, 7498 (2003).
[19] A. K. Singh, T. M. Briere, V. Kumar, and Y. Kawazoe, Phys. Rev. Lett. **91**, 146802 (2000).
[20] A. A. Saranin, A. V. Zotov, V. G. Kotlyar, T. V. Kasyanova, O. A. Utas, H. Okado, M. Katayama, and K. Oura, Nano Lett. **4**, 1469 (2004).
[21] E. Wigner and E. E. Witmer, Z. Phys. **51**, 859 (1928); P. Pechukas and R. N. Zare, Am. J. Phys. **40**, 1687 (1972).
[22] A. N. Andriotis and M. Menon, Phys. Rev. B **60**, 4521 (1999).
[23] A. N. Andriotis, M. Menon, and G. E. Froudakis, Phys. Rev. B **62**, 9867 (2000).
[24] A. E. Frisch, M. J. Frisch, and G. W. Trucks, GAUSSIAN 03 User's Reference, Gaussian Inc., Pittsburgh, PA, 2003.
[25] J. P. Perdew, J. A. Chevary, C. H. Vosko, K. A. Jackson, M. R. Pederson, D. J. Singh, and C. Fiolhais, Phys. Rev. B **46**, 6671 (1992).
[26] J. P. Perdew, K. Burke, and Y. Wang, Phys. Rev. B **54**, 16533 (1996).
[27] A. D. Becke, J. Chem. Phys. **98**, 1372 (1993).
[28] C. Lee, W. Yang, and R. G. Parr, Phys. Rev. B **27**, 785 (1988).
[29] P. J. Hay and W. R. Wadt, J. Chem. Phys. **82**, 270 (1985).
[30] W. R. Wadt and P. J. Hay, J. Chem. Phys. **82**, 284 (1985).
[31] P. J. Hay and W. R. Wadt, J. Chem. Phys. **82**, 299 (1985).
[32] T. H. Dunning, Jr. and P. J. Hay, in *Modern Theoretical Chemistry*, edited by H. F. Schaefer III, Vol. 3 (Plenum, New York, 1976), pp. 1–28.
[33] A. Nicklass, M. Dolg, H. Stoll, and H. Preuss, J. Chem. Phys. **102**, 8942 (1995).
[34] T. Leininger, A. Nicklass, H. Stoll, M. Dolg, and P. Schwerdtfeger, J. Chem. Phys. **105**, 1052 (1996).
[35] X. Y. Cao and M. Dolg, J. Chem. Phys. **115**, 7348 (2001).
[36] P. E. Blöchl, Phys. Rev. B **50**, 17953 (1994).
[37] P. Csaszar and P. Pulay, J. Mol. Struct.: THEOCHEM **114**, 31 (1998).
[38] R. Kishi, H. Kawamata, Y. Negishi, S. Iwata, A. Nakajima, and K. Kaya, J. Chem. Phys. **107**, 10029 (1997).
[39] B. Liu, B. Pen, C. Wang, K. Ho, A. A. Shvartsburg, and M. F. Jarrold, J. Chem. Phys. **109**, 9401 (1998).
[40] A. E. Reed, R. B. Weinstock, and F. Weinhold, J. Chem. Phys. **83**, 735 (1985).
[41] E. D. Glendening, A. E. Reed, J. E. Carpenter, and F. Weinhold, NBO, Version 3.1. See Ref. 22 in detail.
[42] WebElements: http://www.webelements.com/
[43] M. Manninen, J. Mansikka, and E. Hammaren, Europhys. Lett. **15**, 423 (1991).
[44] J. U. Reveles and S. N. Kahanna, Phys. Rev. B **74**, 035435 (2006).